Improved light out-coupling in organic light emitting diodes employing ordered microlens arrays

S. Möller and S. R. Forrest
Department of Electrical Engineering and Princeton Materials Institute, Center for Photonics and Optoelectronic Materials (POEM), Princeton University, Princeton, New Jersey 08544

(Received 5 September 2001; accepted for publication 21 November 2001)

We demonstrate that ordered microlens arrays with 10 μm diam poly-dimethyl-siloxane lenses attached to glass substrates increase the light output of organic light emitting devices (OLED) by a factor of 1.5 over unlensed substrates. The lenses, which are considerably smaller than, and not aligned to the OLEDs, outcouple light that is emitted outside of the escape cone of the substrate. We show that an electrophosphorescent device based on a *fac* tris(2-phenylpyridine)Iridium ($Ir(ppy)_3$) doped emitting layer has its external quantum efficiency increased from 9.5% using a flat glass substrate, to 14.5% at low current densities using a substrate with microlenses. No change in the emission spectrum is observed for different viewing angles using the lens arrays. © *2002 American Institute of Physics.* [DOI: 10.1063/1.1435422]

I. INTRODUCTION

A shortcoming of both inorganic and organic light emitting diodes (referred to as LEDs and OLEDs, respectively) is that only a small fraction of the light generated in the device can escape due to total internal reflection (TIR) in the high refractive index substrates. Light emitted outside of a narrow escape cone suffers TIR as well as waveguiding within the device active layers. Hence almost 80% of the generated light is lost due to waveguiding and TIR in the glass substrates often used in OLEDs.[1] Indeed, the recent demonstration of OLEDs with an external quantum efficiency of η_{ext} of 19%[2,3] indicate that, like LEDs,[4] these devices have an internal quantum efficiency of ~100%. Therefore, methods employed to overcome efficiency limitations due to light trapping concentrate on expanding the escape cone of the substrate and suppressing the waveguide modes. These methods include introducing rough or textured surfaces,[5,6] mesa structures and lenses,[7,8] and the use of reflecting surfaces or distributed Bragg reflectors.[9,10] Furthermore, it has been shown that two dimensional photonic crystals enhance the outcoupling of light along the surface normal.[11,12] Consequently, many of the methods used to improve LED outcoupling have also been applied to OLEDs. For polymer LEDs,[13] it was shown that a corrugated substrate increased the light output by a factor close to 2 by Bragg scattering in the forward direction. A similar improvement was achieved by placing a single millimeter-sized hemispherical lens[1,14] on the substrate aligned with the OLED on its opposite surface. Shaping of the device into a mesa structure also showed an increase of η_{ext} by a factor of 2.[15] The incorporation of monolayers of silica spheres with diameters of 550 nm as a scattering medium in a device, or the positioning of these monolayers on the substrate, also showed enhanced light output.[16] Recently, Tsutsui *et al.* showed that the external quantum efficiency can be doubled by incorporating a thin layer of a very low refractive index silica aerogel ($n \sim 1.03$) in the device.[17] Although a significant increase of η_{ext} was observed for the reported methods, they are often accompanied by changes in the radiation pattern, exhibit an undesirable angle dependent emission spectrum, or employ costly or complex processing methods.

Here we demonstrate an enhancement of the outcoupling efficiency by using an ordered array of microlenses. The lenses are produced using a simple fabrication process, and require no alignment with the OLEDs. Furthermore, the emission spectrum of the lensed OLEDs exhibits no angle dependence. The optical properties of the lens sheets are modeled by a simple ray tracing calculation, which predicts an increase of η_{ext} by a factor of up to 2 compared to an unlensed glass surface. In particular, the light output for high angles of observation with respect to the surface normal is considerably increased. The external quantum efficiency of an electrophosphorescent device is found to increase from 9.5% using a flat glass substrate to 14.5% using a substrate with a micromolded lens array.

II. THEORY OF MICROLENS ARRAY PERFORMANCE

The optical properties of square arrays of hemispherical microlenses with diameters $d=10$ μm can be described by ray optics. A one-dimensional (1D) ray tracing calculation was performed to model the optical properties of the microlenses assuming a typical OLED structure shown in the inset of Fig. 1, grown on a 1 mm thick glass substrate of refractive index $n=1.46$. Indium–tin–oxide (ITO) with a thickness of 150 nm and a refractive index of $n=1.8$ on the glass serves as the anode contact. The organic layers have a total thickness of 100 nm consisting of a hole transport layer (HTL), a light emitting layer (EML), and an electron transport layer (ETL). The refractive indices of the HTL (4,4′-bis[N-(1-naphtyl)-N-phenyl-amino] biphenyl, α-NPD, $n=1.78$) and the ETL (tris(8-hydroxyquinoline) aluminum, Alq_3, $n=1.72$) are taken from the literature.[1] For simplicity the metal cathode is assumed to be an ideal reflector. Micro-

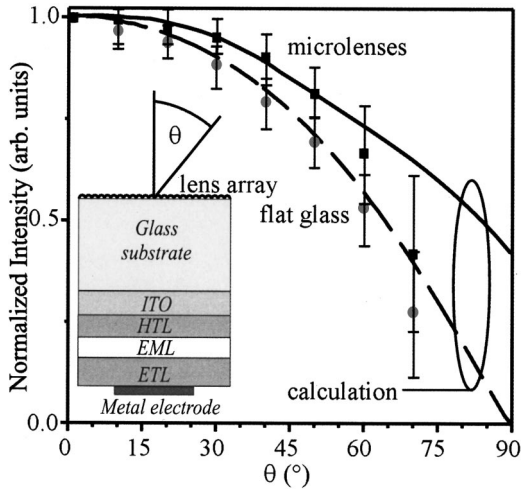

FIG. 1. Calculated (lines) and measured (symbols) radiation patterns of OLEDs with and without microlenses. The lens diameter of both the calculated and fabricated lenses is $d=10$ μm. A glass substrate thickness of 1 mm was used for the calculation for the flat (dashed line) and the lensed substrates (solid line). The inset shows the modeled OLED pixel structure.

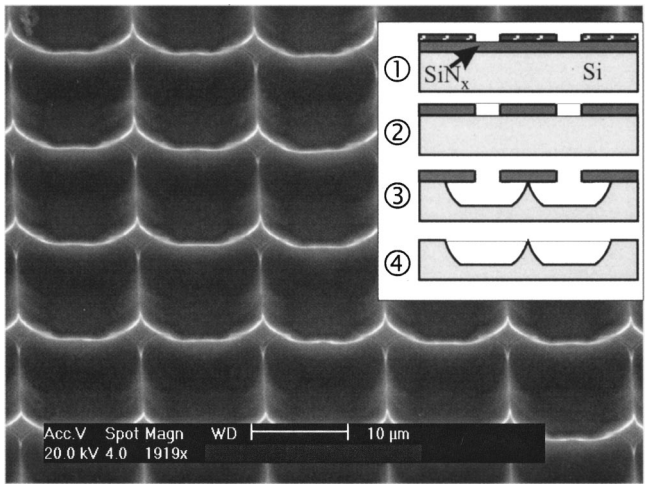

FIG. 2. SEM of the silicon mold used for fabrication of the microlenses. The inset summarizes the fabrication process of the mold. First (steps 1,2) a square hole pattern is etched into a 1 μm thick SiN_x layer on top of a silicon wafer, using photolithography. The Si is then wet etched using the SiN_x as a mask (3). The mold is ready to use after removing the SiN_x (4).

cavity effects and waveguiding are not considered since the microlenses do not significantly affect these processes.

Light generated in the emitting layer under the 1 mm diam circular metal cathode is traced through the device considering refraction at interfaces between layers with different refractive indices. The secondary rays due to Fresnel reflection at these interfaces are also taken into account if their reflected intensity is greater than 0.5%. The rays escaping from the substrate surface in the viewing direction, no more than 10 mm away from the metal cathode, are summed to determine the far field radiation pattern as well as the integrated intensity with and without lenses.

Rays which approach the flat glass substrate at an angle of incidence higher than the critical angle of the glass substrate suffer TIR. When the surface is coated with microlenses, however, the angle of incidence of rays can be smaller than the critical angle leading to their extraction. In addition, the slightly smaller refractive index of the polymer ($n=1.4$) used to fabricate the lenses leads to a greater critical angle compared to that of glass.

Figure 1 shows the calculated far field radiation pattern of an OLED with a flat glass surface (dashed line) and with a microlens array (solid line). For high angles of observation with respect to the substrate surface normal, the microlenses significantly enhance the outcoupling efficiency. To obtain the overall outcoupled intensity, both radiation patterns with and without lenses were integrated over a the viewing half space for angles from $\theta=0°$ to 90°. While this integration is a simplification of the actual optical system which must include microcavity effects, lens array symmetry, deviations from spherical lens shape, and waveguide losses, the value obtained in our calculations can be taken as the upper limit for comparison of the outcoupling efficiency compared with that of a flat glass substrate. The outcoupling efficiency with microlenses is calculated by this means to be increased by a factor of 2.3 compared to the flat glass substrate.

The lens diameter has no significant influence on the extraction efficiency of light from the substrate. However, if the lens diameter is comparable to the size of the device ($d>200$ μm), the radiation pattern shows peaks that correspond to the outcoupling of individual lenses, indicating that alignment of the lenses becomes important in this case. Furthermore, the substrate thickness is important if the microlenses are used for image viewing, e.g., for display applications. Since the microlenses expand the escape cone of the substrate, the illuminated area at the glass–air interface becomes larger. If the substrate is thick, this leads to a large effective pixel size on the outcoupling surface and thus an overlap of the light emitted from adjacent pixels, resulting in a blurred image. Therefore, for image viewing (as opposed to illumination applications) the substrate thickness must not exceed ~0.5 mm without increasing the pixel pitch.

III. LENS FABRICATION

Arrays of microlenses were fabricated using a mold transfer process shown schematically in the inset of Fig. 2. A silicon wafer was coated with a 1 μm thick layer of SiN_x by plasma enhanced chemical vapor deposition. A square hole pattern (6×6 μm) was etched into the SiN_x using standard photolithographic techniques (step 1). After removing the photoresist (2), the Si mold was wet etched in 8:1:1, HNO_3:CH_3COOH:HF using the SiN_x layer as a mask (3). Since the SiN_x is undercut during etching, the shape of the mold depends on the size and shape of the starting pattern. Finally the SiN_x is removed from the silicon wafer by selective etching in HF (4). Figure 2 shows a scanning electron micrograph (SEM) of the silicon mold after removal of the SiN_x. A 400 nm spacing between the $d=10$ μm etched wells is achieved after a 25s Si etch, and the depth of the wells is 4.0×0.1 μm, corresponding to the undercut of the SiN_x by the isotropic etchant.

To fabricate the microlenses, the mold was subsequently filled with poly-dimethyl-siloxane (PDMS), a thermally cur-

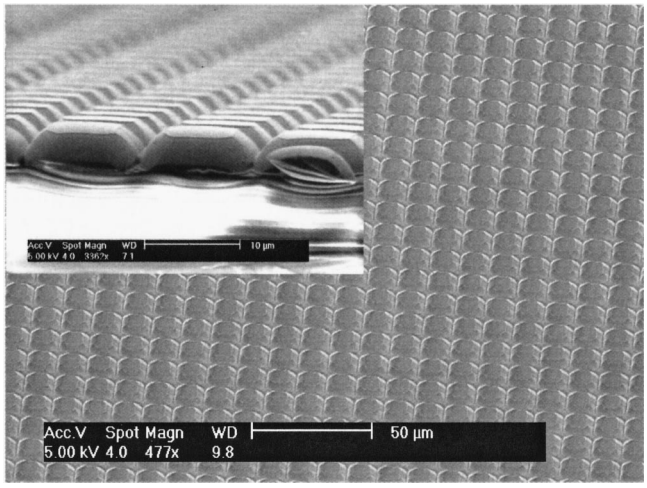

FIG. 3. SEM of a PDMS microlens array fabricated from the mold shown in Fig. 2. The detailed side view of the lenses (inset) shows that the PDMS accurately images the mold shape.

able elastomer. The PDMS is cured at 60 °C for 2 h leading to a flexible sheet that can easily be peeled off of the mold. The thickness of the PDMS layer is typically 100–300 μm. Since PDMS sticks tightly to glass but poorly adheres to Si after it is cured, the PDMS precursor can be confined between the mold and a glass substrate. After curing, the PDMS remains on the glass substrate when the latter is separated from the mold. As shown in Fig. 3, this leads to a very thin PDMS sheet with lenses (diameter $d \sim 10$ μm). Large areas can be covered with an ordered array of microlenses, limited only by the size of the mold. A magnified image of the lenses (inset, Fig. 3) confirms that PDMS accurately reproduces the mold shape.

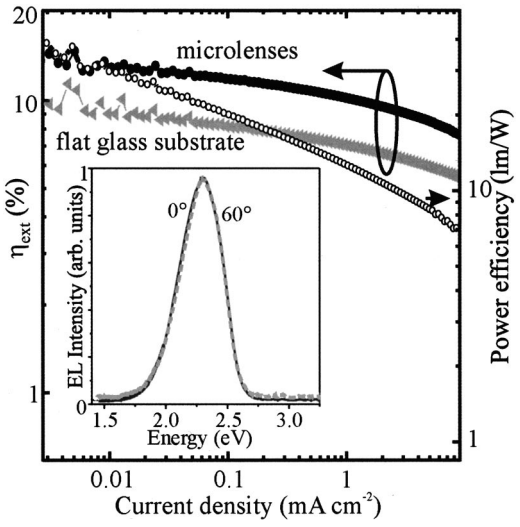

FIG. 4. External quantum η_{ext} and power efficiency vs current density of an $Ir(ppy)_3$ doped phosphorescent OLED. When lenses are attached to the substrate, η_{ext} is increased by 50% at all current densities, when compared to a flat glass substrate. (Inset) Spectra of the OLED measured parallel to (solid line), and 60° from (dashed line) the surface normal.

IV. APPLICATION TO OLEDs

To determine the effects of the microlens arrays, they were attached to OLEDs previously fabricated on flat glass substrates. The organic layers of the OLEDs were deposited by high vacuum (base pressure $\sim 10^{-6}$ Torr) thermal evaporation onto a cleaned glass substrate precoated with an ITO layer with a sheet resistance of $\sim 20\ \Omega/\square$. A 50 nm thick film of 4,4′-bis[N,N′-(3-tolyl)amino]-3,3-dimethylbiphenyl (HMTPD) served as the HTL. The EML consisted of 6%–8% of the phosphor, *fac* tris(2-phenylpyridine)iridium ($Ir(ppy)_3$), doped into the electron-transporting 3-phenyl-4-(1′-naphthyl)-5-phenyl-1,24-triazole (TAZ) via thermal coevaporation. A 40 nm thick ETL of tris(8-hydroxyquinoline)aluminum (Alq_3) was used to transport and inject electrons into the EML. A shadow mask with 1 mm diam openings was used to define the cathode contact consisting of a 75 nm thick Mg–Ag layer with a 75 nm thick Ag cap layer. In past reports, similar Mg:Ag/Alq_3/$Ir(ppy)_3$:TAZ/HMTPD/ITO devices deposited onto flat glass substrates have exhibited external quantum efficiencies as high as $\eta_{ext} = 19\%$.[2]

Figure 4 shows η_{ext} versus current density for devices with and without the microlenses attached to the substrate surface. The efficiency η_{ext} of the device without lenses is 9.5% at a current density of 0.1 mA/cm^2, whereas attachment of the lenses leads to an increase of η_{ext} by a factor of 1.5, to 14.5%. A peak luminous power of 35 lm/W is achieved for these OLEDs. The radiation pattern (symbols in Fig. 1) of the OLED with and without lenses show that the lenses enhanced the light outcoupling as predicted in our 1D calculations. Since the sample holder partially shaded the photodetector for high angles ($<60°$) the data fall below the calculated values. In addition, while the best case 2D integration predicts a maximum increase in intensity of 2.3, which exceeds our measured value of 1.5, this difference is primarily attributed to the use of a square array of microlenses whose shape deviates markedly from hemispherical.

As expected, the light intensity is enhanced particularly at high viewing angles with respect to the substrate normal as compared to the flat glass surface. The spectra of the OLED with microlenses parallel to (solid line) and 60° from the substrate normal (dashed line) are shown in the inset of Fig. 4. The spectrum does not vary with viewing angle, confirming that the microlenses simply redirect the light without introducing microcavities or other undesirable parasitic optical effects.

As noted above, the application to high resolution displays requires that the substrate and the lens sheet are thin ($\sim$0.5 mm) to avoid image blurring. To qualitatively assess the image quality expected from the use of such lens arrays, Fig. 5(b) shows a photograph of a lens sheet on a glass substrate with a combined thickness of 350 μm, placed on top of text printed in different font sizes on a 600 dpi laser printer. For comparison, Fig. 5(a) shows the same printout without the substrate and lenses. The edges of the letters underneath the microlenses are slightly blurred in this magnified photograph, but even the smallest letters (3 point$\cong$1.5 mm), which are barely resolvable in their original sizes on

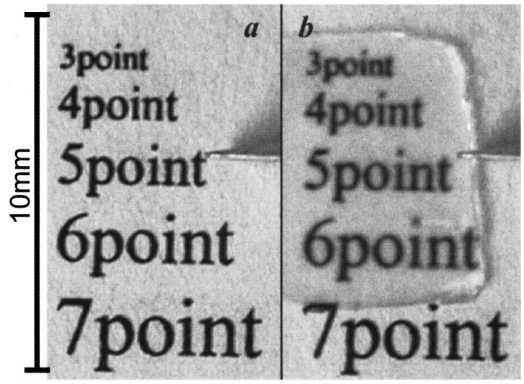

FIG. 5. Photoograph of text printed in different point sizes on a 600 dpi laser printer. The photograph (a) shows the plain paper printout, while (b) shows the printout covered with a lens sheet and glass substrate with a total thickness of 350 μm.

any conventional monitor, are clearly resolved here. This indicates that the microlens arrays can be applied to displays if the substrate and lens sheet thickness are optimized. Image blurring is completely eliminated even for the smallest fonts if the lens sheet is placed directly on the surface of top emitting OLEDs.[18]

Image resolution is not a relevant consideration for large area OLEDs employed in lighting applications, when image viewing is not required. The enhanced extraction efficiency of light out of the glass substrate of a 2.5 cm×2.5 cm OLED by attaching a microlens sheet is shown in the photograph taken at an angle of about 45° in Fig. 6. The area of the OLED which is covered by the lens sheet is significantly brighter than the uncovered area, especially for high angles of observation. Light is scattered at the rough edges of the PDMS lens sheet shown in Fig. 6. This results in bright edges, which are reflected at the bottom surface of the supporting glass substrate of the OLED and can be seen as a mirror image below the lens sheet.

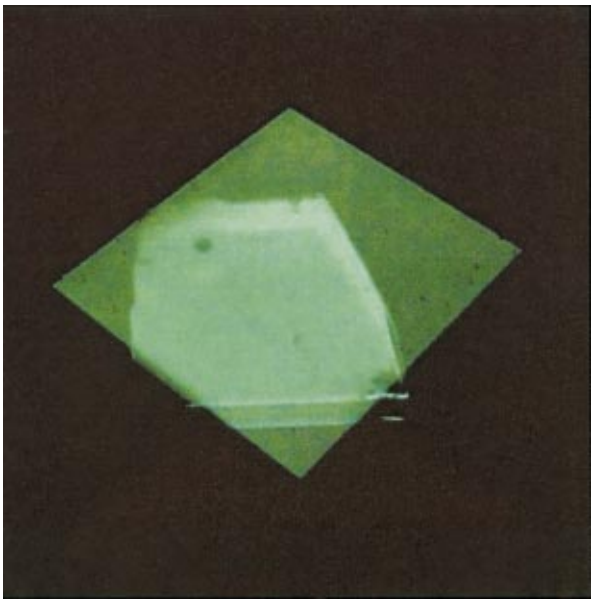

FIG. 6. (Color) Photograph of a large area OLED (2.5 cm×2.5 cm) which is partly covered by a PDMS lens sheet. The covered area is significantly brighter than the uncovered regions, demonstrating the enhanced extraction of light out of the substrate using the microlenses.

V. CONCLUSION

We have shown that microlens arrays increase the external quantum efficiency of OLEDs by a factor of at least 1.5, resulting in a considerable decrease in power consumption to achieve a particular emission intensity. The 50% increase in η_{ext} agrees with estimations obtained from a simple ray tracing model that ignores waveguiding and other optical losses. The microlenses primarily widen the escape cone for total internally reflected light incident at the air–substrate boundary. Thus the extraction of light at angles higher than the critical angle of glass is enhanced. Since the lens diameters are ~10 μm, no color changes of the spectrum are observed. Furthermore the dense packing of the microlenses makes alignment with the OLEDs unnecessary. The fabrication process by molding allow for simple and large area fabrication, making these arrays applicable to lighting as well as display applications.

ACKNOWLEDGMENTS

The authors gratefully acknowledge Universal Display Corporation and DARPA for their support of this work. They also thank Professor Chihaya Adachi for valuable discussions.

[1] V. Bulovic, V. B. Khalfin, G. Gu, P. E. Burrows, D. Z. Garbuzov, and S. R. Forrest, Phys. Rev. B **58**, 3730 (1998).
[2] C. Adachi, M. Baldo, S. R. Forrest, and M. E. Thompson, J. Appl. Phys. **90**, 5048 (2001).
[3] M. Ikai, S. Tokito, Y. Sakamoto, T. Suzuki, and Y. Taga, Appl. Phys. Lett. **79**, 156 (2001).
[4] R. J. Nelson and R. G. Sobers, J. Appl. Phys. **49**, 6103 (1978).
[5] A. A. Bergh and R. H. Saul, US Patent No. 3,739,217 (1973).
[6] I. Schnitzer, E. Yablonovitch, C. Caneau, T. J. Gmitter, and A. Scherer, Appl. Phys. Lett. **63**, 2174 (1993).
[7] R. H. Haitz, US Patent No. 5,087,949 (1992).
[8] R. Windisch, P. Heremans, A. Knobloch, P. Kiesel, G. H. Dohler, B. Dutta, and G. Borghs, Appl. Phys. Lett. **74**, 2256 (1999).
[9] I. Schnitzer, E. Yablonovitch, C. Caneau, and T. J. Gmitter, Appl. Phys. Lett. **62**, 131 (1993).
[10] F. A. Kish, Jr. and S. A. Stockman, US Patent No. 6,015,719 (2000).
[11] S. H. Fan, P. R. Villeneuve, J. D. Joannopoulos, and E. F. Schubert, Phys. Rev. Lett. **78**, 3294 (1997).
[12] M. Boroditsky, R. Vrijen, T. F. Krauss, R. Coccioli, R. Bhat, and E. Yablonovitch, J. Lightwave Technol. **17**, 2096 (1999).
[13] B. J. Matterson, J. M. Lupton, A. F. Safonov, M. G. Salt, W. L. Barnes, and I. D. W. Samuel, Adv. Mater. **13**, 123 (2001).
[14] C. F. Madigan, M. H. Lu, and J. C. Sturm, Appl. Phys. Lett. **76**, 1650 (2000).
[15] G. Gu, D. Z. Garbuzov, P. E. Burrows, S. Venkatesh, S. R. Forrest, and M. E. Thompson, Opt. Lett. **22**, 396 (1997).
[16] T. Yamasaki, K. Sumioka, and T. Tsutsui, Appl. Phys. Lett. **76**, 1243 (2000).
[17] T. Tsutsui, M. Yahiro, H. Yokogawa, K. Kawano, and M. Yokoyama, Adv. Mater. **13**, 1149 (2001).
[18] V. Bulovic, G. Gu, P. E. Burrows, S. R. Forrest, and M. E. Thompson, Nature (London) **380**, 29 (1996).